NEURAL REGENERATION RESEARCH
May 2014, Volume 9, Issue 10
www.nrronline.org

# Analgesic effect of intrathecal bumetanide is accompanied by changes in spinal sodium-potassium-chloride co-transporter 1 and potassium-chloride co-transporter 2 expression in a rat model of incisional pain

**Yanbing He[1, 2], Shiyuan Xu[1], Junjie Huang[2], Qingjuan Gong[2]**

1 Department of Anesthesiology, Zhujiang Hospital, Southern Medical University, Guangzhou, Guangdong Province, China
2 Department of Anesthesiology and Pain Medicine, the Second Affiliated Hospital of Guangzhou Medical University, Guangzhou, Guangdong Province, China

***Corresponding author:***
*Shiyuan Xu, M.D., Department of Anesthesiology, Zhujiang Hospital, Southern Medical University, Guangzhou, Guangdong Province, China, xushiyuan355@163.com.*

***doi:****10.4103/1673-5374.133170*
***http:****//www.nrronline.org/*

***Accepted:*** *2014-03-10*

## Abstract

Accumulating evidence has demonstrated that the sodium-potassium-chloride co-transporter 1 and potassium-chloride co-transporter 2 have a role in the modulation of pain transmission at the spinal level through chloride regulation in the pain pathway and by effecting neuronal excitability and pain sensitization. The present study aimed to investigate the analgesic effect of the specific sodium-potassium-chloride co-transporter 1 inhibitor bumetanide, and the change in spinal sodium-potassium-chloride co-transporter 1 and potassium-chloride co-transporter 2 expression in a rat model of incisional pain. Results showed that intrathecal bumetanide could decrease cumulative pain scores, and could increase thermal and mechanical pain thresholds in a rat model of incisional pain. Sodium-potassium-chloride co-transporter 1 expression increased in neurons from dorsal root ganglion and the deep laminae of the ipsilateral dorsal horn following incision. By contrast, potassium-chloride co-transporter 2 expression decreased in neurons of the deep laminae from the ipsilateral dorsal horn. These findings suggest that spinal sodium-potassium-chloride co-transporter 1 expression was up-regulated and spinal potassium-chloride co-transporter 2 expression was down-regulated following incision. Intrathecal bumetanide has analgesic effects on incisional pain through inhibition of sodium-potassium-chloride co-transporter 1.

***Key Words:*** *nerve regeneration; sodium-potassium-chloride co-transporter 1; potassium-chloride co-transporter 2; bumetanide; spinal cord; dorsal root ganglion; incision model; postoperative pain; neural regeneration*

***Funding:*** *This study was supported by a grant from Guangzhou Medical University, No. 2008C24.*

*He YB, Xu SY, Huang JJ, Gong QJ. Analgesic effect of intrathecal bumetanide is accompanied by changes in spinal sodium-potassium-chloride co-transporter 1 and potassium-chloride co-transporter 2 expression in a rat model of incisional pain. Neural Regen Res. 2014;9(10):1055-1062.*

## Introduction

Despite advances in analgesic drugs and other pain therapies, postoperative pain remains a common clinical problem (Brennan, 2011; Wu and Raja, 2011). Many patients suffering from moderate to severe pain after surgery may develop a chronic pain syndrome. The chronic pain syndrome is usually neuropathic, with apoptosis of inhibitory neurons and regeneration of excitatory neurons or abnormal synapses, and is difficult to treat (Bolay and Moskowitz, 2002). The estimated incidences of chronic pain after various procedures, including leg amputation, thoracotomy, breast surgery, cholecystectomy, and inguinal herniorrhaphy, range from about 10% to 60% (Aasvang and Kehlet, 2005; Kehlet et al., 2006). The intensity of acute postoperative pain correlates with the risk of developing chronic pain (Lavand'homme, 2006), highlighting the importance of early aggressive therapy.

The lack of success in treating postoperative pain and preventing the transition to a chronic pain syndrome stems, at least in part, from our poor understanding of the pathophysiology of postoperative pain (Lavand'homme, 2006; Brennan, 2011). The rat incision model first reported by Brennan et al. in 1996 is one of the most common animal models for mechanistic research on postoperative pain (Brennan et al., 1996). Studies using this model suggest that post-incision pain differs mechanistically from inflammatory or neuropathic pain, and that central sensitization probably contributes to postoperative pain following surgical incision (Zahn et al., 2002a). Current treatments focus mainly on blocking neurotransmission in pain pathways, but this strategy has achieved only limited success. The use of opioids is limited by its side effects like nausea, vomiting, respiratory depression, and sedation. Moreover, opioid-induced hyperalgesia can occur after high doses of opioids perioperatively (Wu and Raja, 2011). So the combination of both analgesic and

anti-hyperalgesic drugs should be administrated for "balanced analgesia". Recently, gabapentinoids that are able to modulate central sensitization have been trialed for postoperative pain. Systematic reviews of randomized controlled trials suggest that use of gabapentin will decrease postoperative pain, but might be associated with an increased incidence of sedation (Vadivelu et al., 2010; Imani and Rahimzadeh, 2012). Therefore, developing a novel analgesic agent without side effects on consciousness and sensation to non-pain stimulation is important for postoperative pain treatment.

Cation-chloride cotransporters (CCCs) are a class of membrane proteins that transport sodium, potassium, and chloride ions into and out of cells (Haas and Forbush, 1998). Sodium-potassium-chloride co-transporter 1 (NKCC1) and potassium-chloride co-transporter 2 (KCC2) are two major CCC subtypes that regulate chloride balance within the nervous system. Under physiological conditions, NKCC1 transports $Cl^-$ into the cell whereas KCC2 transports $Cl^-$ out of the cell (Payne et al., 2003; Blaesse, 2009). Both transporters contribute to the anion equilibrium potential (Eanion) in pain pathway neurons, thus influencing neural excitability and pain sensitization (Price et al., 2005; Price et al., 2009; Chamma et al., 2012). Changes in NKCC1 and KCC2 expression levels have been reported in both inflammatory and neuropathic pain models. Moreover, the CCC inhibitors furosemide and bumetanide are effective antinociceptive agents in these models (Granados-Soto et al., 2005; Zhang et al., 2008; Hasbargen et al., 2010).

In our previous study, we found that intrathecal furosemide reduced both primary and secondary hyperalgesia in a rat model of incisional pain, suggesting that changes in CCC function do indeed contribute to postoperative pain and sensitization (He et al., 2011). However, abnormal excitatory behavior was seen after intrathecal furosemide was administered to intact and incision rats, which might be caused by blocking of KCC2 (He et al., 2011). Since bumetanide is a specific NKCC1 inhibitor that has about 500-fold greater affinity for NKCC1 than for KCC2 (Blaesse, 2009), in the present study we evaluated the analgesic effect of intrathecal bumetanide, measured evoked and non-evoked pain behaviors, and determined changes in NKCC1 and KCC2 protein expression in a rat model of incisional pain. Our goal was to gain insights into the effectiveness of NKCC1 blockers for postoperative pain treatment.

## Materials and Methods

### Animals

Experiments were performed on 66 adult male Sprague-Dawley rats, aged 8–10 weeks and weighing 250–300 g that were purchased from Guangdong Medical Laboratory Animal Center (Animal license No. 0078910). Rats were housed in pairs in plastic cages with soft bedding under a 12-hour light-dark cycle with food and water *ad libitum*. All procedures were approved by the Animal Care Committee of Guangzhou Medical University in China and conducted in accordance with the Guidelines of the National Institutes of Health on Animal Care and the Ethical Guidelines for Investigation of Experimental Pain in Conscious Animals. Efforts were made to minimize animal suffering and the number of animals used.

### Grouping

Thirty-six rats were randomly and evenly divided into a control group and a bumetanide group for behavior measurements. In the bumetanide group, 100 μg/20 μL bumetanide solution was intrathecally injected prior to incision. In the control group, only 20 μL artificial cerebral spinal fluid was intrathecally injected prior to incision. Rats were then measured for cumulative pain score, thermal withdrawal latency, and mechanical pain threshold ($n = 6$ for each group). Another 30 adult male Sprague-Dawley rats (without bumetanide administration) were randomly divided into one control group and four incision groups (2 hours, 2, 3 and 6 days post-incision; $n = 6$ for each group) for immunohistochemical measurements of NKCC1 and KCC2.

### Drug preparation and administration

Bumetanide (Sigma, St. Louis, MO, USA, B3023) was dissolved in 5 μg/μL artificial cerebrospinal fluid vehicle (Department of Anesthesiology, Zhujiang Hospital, Southern Medical University, Guangzhou, China). The artificial cerebrospinal fluid vehicle (pH 7.2–7.4) was composed of (in mmol/L) 1.3 $CaCl_2 \cdot 2H_2O$, 2.6 KCl, 0.9 $MgCl_2$, 21.0 $NaHCO_3$, 2.5 $Na_2HPO_4 \cdot 7H_2O$, 125.0 NaCl, and 3.5 dextrose. Bumetanide was injected under inhalation anesthesia. Anesthesia was induced by 3% isoflurane inhalation in an induction chamber and maintained by 2.5% *via* a nose cone with 0.3 L/min oxygen. The back was shaved, and the drug was injected into the intrathecal space at the $L_{3-4}$ interspace (with the positive indication being tail movement). A 30-gauge needle (Hamilton 7748-16) connected to a 50-μL syringe (Hamilton 705LT) was employed with the rat in the elevated lumbar position.

### Preparation of rat models of incisional pain

The incision model was created according to a previously reported method (Zahn et al., 2002b). Briefly, under inhalation anesthesia, the plantar aspect of the left hindpaw was sterilized and a 1-cm longitudinal incision was made through the skin and fascia, including the plantaris muscle, starting 0.5 cm from the proximal edge of the heel and extending toward the toes. The skin was then apposed using two 4–0 antibacterial absorbable sutures.

### Pain behavior measurements

*Cumulative pain score*

Rats for cumulative pain score measurement were placed on an elevated plastic mesh floor (grid 8 mm × 8 mm) under a clear plastic cage, using an angled magnifying mirror to view the incised foot. Following 20 minutes' adaptation, each rat was closely observed during a 1-minute period, once every 5 minutes for 1 hour. Depending on the position in which the foot was found, 0, 1, or 2 was given. If full weight bearing of the foot was present and the wound was blanched or distort-

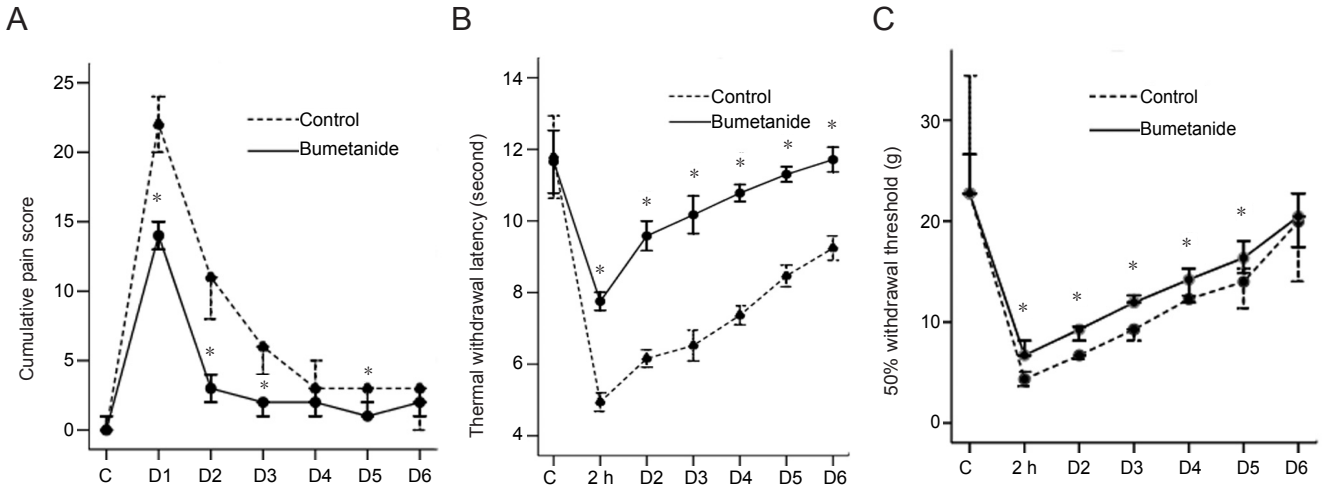


**Figure 1 Intrathecal bumetanide alleviated rat incisional pain.**
(A–C) The control (C) group received intrathecal artificial cerebral spinal fluid vehicle (20 μL) just prior to incision. The bumetanide group received intrathecal bumetanide (100 μg/20 μL) just prior to incision. Data were expressed as mean ± SD. $n = 6$, $*P < 0.05$, *vs.* control group. (A) Intrathecal bumetanide decreased cumulative pain score following incision. The cumulative pain score was between 0 and 24 according to the degree of rest pain. D1 through to D6 represented the first to sixth days after incision, respectively. Data are presented as median and interquartile range and Mann-Whitney *U* test was used to compare the cumulative pain scores between groups. (B) Intrathecal bumetanide increased thermal withdrawal latency following incision. Paw withdrawal latency time was recorded as the average of three trials using the withdrawal test to a thermal noxious stimulus. D1 through to D6 represented the first to sixth days after incision, respectively. Two-sample *t* test was used to compare the thermal withdrawal latencies between groups. (C) Intrathecal bumetanide increased 50% probability withdrawal threshold following incision. The 50% probability withdrawal threshold was determined using the modified up-down method of Dixon. D1 through to D6 represented the first to sixth days after incision, respectively. Data are presented as median and interquartile range and Mann-Whitney *U* test was used to compare the 50% probability withdrawal thresholds between groups.

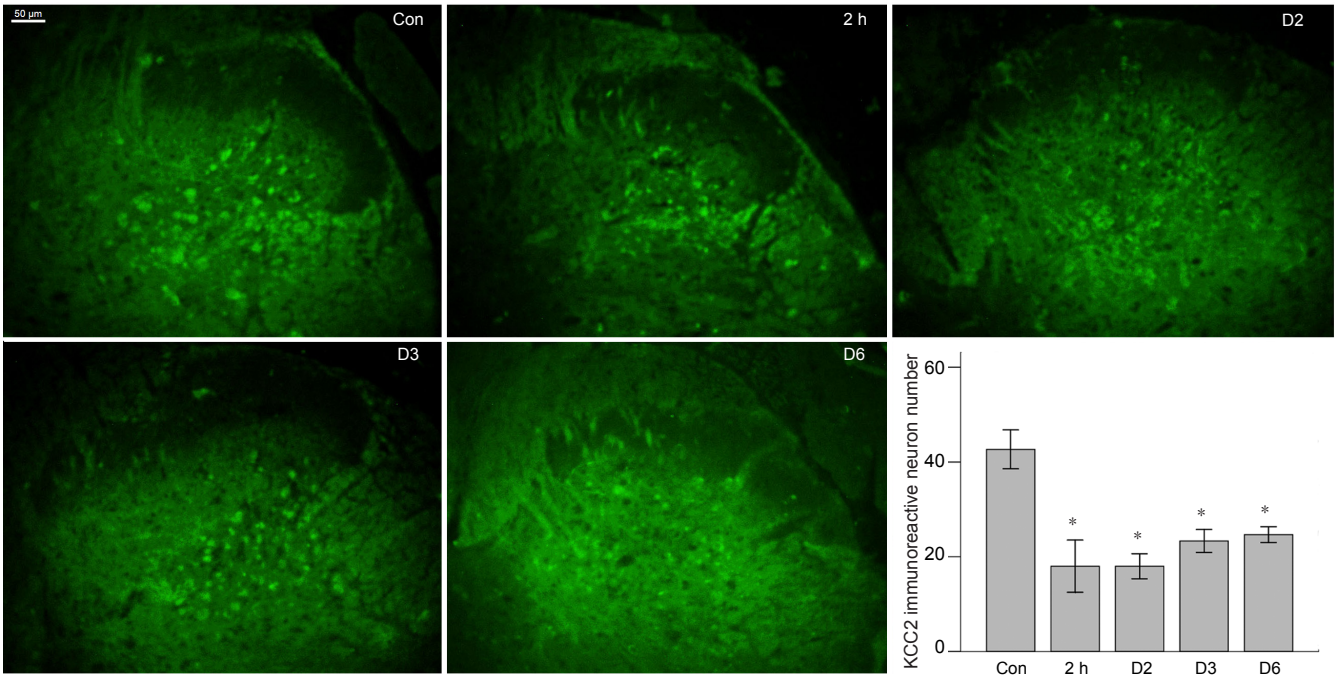


**Figure 3 Potassium-chloride co-transporter 2 (KCC2) expression decreased in the deep laminae of ipsilateral dorsal horn of $L_{4–5}$ spinal cord after incision.**
KCC2 immunoreactivity was indicated by fluorescein isothiocyaute (FITC)-conjugated IgG (green). Control group (Con): Significant KCC2 immunoreactivity was observed in the deep layers of dorsal horn in intact rats. 2 hours, 2, 3 and 6 days post-incision groups (2 h, D2, D3, D6): KCC2 immunoreactivity decreased in the deep layers of ipsilateral dorsal horn at 2 hours, 2, 3 and 6 days following incision, but increased in the substantia gelatinosa layer. Scale bar: 50 μm. Right bottom: KCC2 immunoreactive neuron quantification in the ipsilateral deep layers of dorsal horn of $L_{4–5}$ spinal cord ($n = 6$). One-way analysis of variance followed by Levene's *post hoc* test was used for pairwise comparisons. Data were expressed as mean ± SD. $n = 6$, $*P < 0.05$, *vs.* control group.

ed by the mesh, a score of 0 was recorded. If the area of the wound touched the mesh without blanching or distorting, a score of 1 was given. If the foot was completely off the mesh, a score of 2 was recorded. The sum of the 12 scores (0–24) obtained during the 1-hour session was used to assess pain in the incised foot (Zahn et al., 1998). Rats of the control and bumetanide groups ($n = 6$ for each group) were observed for 1 hour per day and the total score was recorded to represent the degree of rest pain.

*Thermal withdrawal latency*

Thermal pain threshold was assessed using the hind paw withdrawal test after a thermal noxious stimulus. Briefly, a radiant heat source beneath a glass floor was aimed at the plantar surface, which was 0.5 mm away from the wound of the hind paw. Paw withdrawal latency time was recorded as the average of three trials with intervals greater than 5 minutes (Hargreaves et al., 1988). Rats of the control and bumetanide groups ($n = 6$ for each group) were tested once per day and the withdrawal latency time (WLT) was recorded as seconds to represent the thermal pain threshold.

*Mechanical pain threshold*

After 2 days of adaptation to the measuring cage, measurement was started on the third day. First, the rat was placed in the measuring cage for more than half an hour to acclimate. Then, baseline pain behavior was evaluated. To assess the hindpaw withdrawal threshold to a mechanical stimulus, von Frey filaments of logarithmic incremental stiffness (0.6–26.0 g) were used, and 50% probability withdrawal thresholds were calculated. The experiment was not begun until the baseline was above 20 (the experiment being performed on the next day after this criterion was satisfied). The 50% withdrawal threshold was determined using the modified up-down method of Dixon. The calculation was performed using the formula: 50% g threshold = $(10[Xf + k\delta])/10{,}000$ where $Xf$ = value (in log units) of the final von Frey hair used; $k$ = tabular value for the pattern of positive/negative responses; and $\delta$ = mean difference (in log units) between stimuli (Chaplan et al., 1994). The three pain behavior tests were performed separately before incision (con), 2 hours post-incision, and 2 to 6 days post-incision (2 h, 2 d, 3 d, 6 d post-incision).

**Immunohistochemistry**

At different time points before and after incision (con, 2 h, 2 d, 3 d, 6 d post-incision), under deep anesthesia with 5% sodium pentobarbital (about 100 mg/kg), rats were perfused through the ascending aorta with PBS followed by paraformaldehyde at 4°C. The $L_{4–5}$ spinal cord segments and bilateral $L_5$ dorsal root ganglia were carefully removed. Each dorsal root ganglia was post-fixed for 25 minutes and spinal cord segments for 14 hours in the same fixative. Fixed tissues were then sequentially dehydrated in 10%, 20%, and 30% sucrose over three successive nights at 4°C. Five group samples were arranged on the same blocks in optimal cutting temperature embedding medium (Tissue-Tek, Leica, Nussloch, Germany) and mounted on the same slides after sectioning. Transverse spinal sections (16 μmol/L) were cut on a cryostat (Leica CM 1950) and processed for NKCC1 or KCC2 immunostaining. Briefly, slices were blocked in 5% ChemiBLOCKER™ (Millipore Corporation, Billerica, MA, USA) and 0.5% Triton X100 in PBS for 1 hour at room temperature. Primary antibodies were diluted in the same buffer. For dorsal root ganglion immunostaining, fixed tissues were incubated in primary polyclonal antibody (goat anti-NKCC1, Santa Cruz Biotechnology, #sc-21545; goat anti-KCC2, Santa Cruz Biotechnology, #sc-19420; 1:20) for 2 hours at room temperature. For spinal cord immunostaining, slices were incubated over two nights at 4°C with the same antibody (1:100). After three washes in PBS, sections were incubated for 90 minutes with FITC-conjugated donkey anti-goat IgG (Jackson ImmunoResearch Inc., 705-095-003, 1:200), and 4′,6-diamidino-2-phenylindole (DAPI; 0.3 μmol/L) was used to stain the nuclei in the last 10 minutes. For double staining with neuronal markers, rabbit anti-neurofilament 200 (NF 200; Sigma, N4142, 1:400) and AMCA conjugated donkey anti-goat IgG (Jackson ImmunoResearch Inc., 705-155-147; 1:300), TRITC-conjugated donkey anti-rabbit IgG (Jackson ImmunoResearch Inc., 711-025-152; 1:300), and FITC-conjugated lectin B4 (Sigma, St. Louis, MO, USA; L2895; 3.3 μg/mL) were used. Slides were analyzed using an inverted microscope (Leica DM IL, Wetzlar, Germany) equipped with a Leica DFC425C CCD camera and Leica LAS software, and immunoreactive neurons were counted. No immunosignal was observed upon omission of primary antibody and preadsorption control using a fivefold excess of blocking peptides according to the manufacturer's specification. NKCC1 or KCC2 immunoreactive neuron numbers were counted in three discontinuous slices per rat and the mean number was recorded to represent the expression level.

**Statistical analysis**

Statistical data were analyzed using the SPSS 16.0 software (SPSS, Chicago, IL, USA). The results of 50% withdrawal threshold and cumulative pain score were presented as median and interquartile range. The data between testing days within groups were analyzed using Friedman test, followed by Wilcoxon matched pairs test, while the Mann-Whitney $U$ test was used between groups. The results of WLT were presented as mean ± SD, and the two-sample $t$ test was used between and within groups. For neuron quantification, group means were compared by one-way analysis of variance followed by Levene's *post hoc* test for pairwise comparisons, and significance was determined as $P < 0.05$.

## Results

**Intrathecal bumetanide decreased cumulative pain scores in a rat model of incisional pain**

Both in the control and bumetanide groups, the cumulative pain scores were significantly increased following incision ($P < 0.001$). There was no significant difference in baseline scores between these two groups ($P > 0.05$). However, after incision, the scores of the bumetanide group were significant-

ly lower than the control group ($P < 0.01$ for days 1, 2, 3, 5 post-incision groups). The difference on days 4 and 5 post-incision was not significant ($P > 0.05$; **Figure 1A**).

**Intrathecal bumetanide increased thermal pain threshold in a rat model of incisional pain**

In the control group, from 2 hours to the sixth day after incision, the thermal withdrawal latencies were significantly lower than baseline ($P < 0.01$). However, in the bumetanide group, from only 2 hours to the third day after incision, the thermal withdrawal latencies were significantly lower than baseline ($P < 0.05$). The baseline withdrawal latency time of the two groups showed no difference ($P > 0.05$), but from 2 hours to the sixth day after incision, the thermal withdrawal latencies of the bumetanide group were significantly higher than the control group (all $P < 0.01$; **Figure 1B**).

**Intrathecal bumetanide increased mechanical pain threshold in a rat model of incisional pain**

Both in the control and bumetanide groups, the 50% withdrawal thresholds were significantly decreased from 2 hours to the sixth day following incision (all $P < 0.05$). There was no significant difference in basement threshold between the control and bumetanide groups ($P > 0.05$). However, from 2 hours to the fifth day after incision, the thresholds of the bumetanide group were significantly higher than the control group ($P < 0.05$). On the sixth day, the difference was not significantly different ($P > 0.05$; **Figure 1C**).

**NKCC1 expression increased in dorsal root ganglion and dorsal horn of spinal cord following incision**

In intact rats, NKCC1 was weakly expressed in dorsal root ganglion and dorsal horn (**Figure 2 con**). After incision, NKCC1 expression increased in bilateral dorsal root ganglia, with a greater increase in the ipsilateral dorsal root ganglion. NKCC1 immunoreactivity was found mainly on the neuronal membrane (**Figure 2A**). The number of NKCC1 immunoreactive neurons in the ipsilateral dorsal root ganglion increased from 2 hours to 3 days following incision ($P < 0.05$; **Figure 2B**). In the ipsilateral dorsal horn, NKCC1 immunoreactivity increased in the deep layers, and weak NKCC1 immunoreactivity was observed in the substantia gelatinosa (SG). NKCC1 immunoreactivity was not observed in the control group rats (**Figure 2C**). The number of NKCC1 immunoreactive neurons in the ipsilateral dorsal horn increased at 3 and 6 days after incision ($P < 0.01$; **Figure 2D**).

**KCC2 expression decreased in ipsilateral dorsal horn following incision**

No significant KCC2 immunoreactivity was found in the dorsal root ganglion. In control rats, KCC2 was predominantly expressed in the deep laminae of the dorsal root, appearing much stronger than NKCC1 expression. There was little detectable KCC2 expression in the SG. After incision, KCC2 immunoreactivity decreased in the deep laminae of the ipsilateral dorsal horn, although the KCC2 immunoreactivity increased in SG, and the number of KCC2 immunoreactive neurons in the deep laminae was significantly lower than controls from 2 hours to 6 days following incision (all $P < 0.01$; **Figure 3**).

**NKCC1 was significantly expressed in C-fiber neurons in dorsal root ganglion, and both NKCC1 and KCC2 were predominantly expressed in A-fiber neurons in the dorsal horn**

Double staining for NKCC1 and the C-fiber afferent neuron marker Isolectin B4 (IB4) in dorsal root ganglion demonstrated that NKCC1 immunoreactivity was most significantly observed in C-fiber neurons than other larger diameter cells (**Figure 4A**). Double staining of NKCC1 and the A-fiber afferent neuron marker neurofilament 200 (NF200) in the dorsal horn revealed that NKCC1 was significantly expressed in A-fiber neurons in deep layers (**Figure 4B**). Co-staining of KCC2 and NF200 in dorsal horn showed that KCC2 was predominantly expressed in deep A-fiber neurons (**Figure 4C**).

## Discussion

The present study revealed that intrathecal bumetanide could improve guarding pain behavior, and heat and mechanical hyperalgesia following incision in rats. Immunohistochemistry results showed that spinal NKCC1 expression was increased whereas spinal KCC2 expression decreased following incision.

We measured both the evoked pain behavior (thermal withdrawal latencies and mechanical pain threshold) and the non-evoked pain behavior (cumulative pain scores) to evaluate the analgesic effect of intrathecal bumetanide. Mechanical and heat stimuli can be used to largely evaluate cutaneous sensitivity after incision, but fail to reflect ongoing activity in nociceptive pathways, which relate to pain at rest (Brennan, 2011). Results suggested that bumetanide was effective in both rest pain and evoked pain and was a promising analgesic drug for postoperative pain. Compared with the results of intrathecal furosemide in the rat model of incisional pain in our last report (He et al., 2011), we obtained a similar antinociceptive effect, and no abnormal excitatory behavior was found. We suggested that the NKCC1 selective blocker was safer than the blocker of both NKCC1 and KCC2.

The paucity of reliable antibodies for the detection of NKCC1 and KCC2 in the spinal cord and dorsal root ganglion has led many to use PCR or western blotting to measure expression (Price et al., 2009). We used the method from Funk and Gilbert (Gilbert et al., 2007; Funk et al., 2008), and succeeded in showing protein expression in the spinal cord and dorsal root ganglion, although the figures were not perfect. To illuminate the expression of NKCC1/KCC2 in neurons and investigate subtypes of sensory neurons, co-staining with two neuron markers, IB4 and NF200, was also performed. NKCC1 mRNA expression has been reported to be largely confined to small- and medium-diameter dorsal root ganglion neurons (Price et al., 2006), but we found that NKCC1 immunoreactivity was present in almost all dorsal root ganglion neurons, including large-diameter neurons. According to the result of double staining with NKCC1

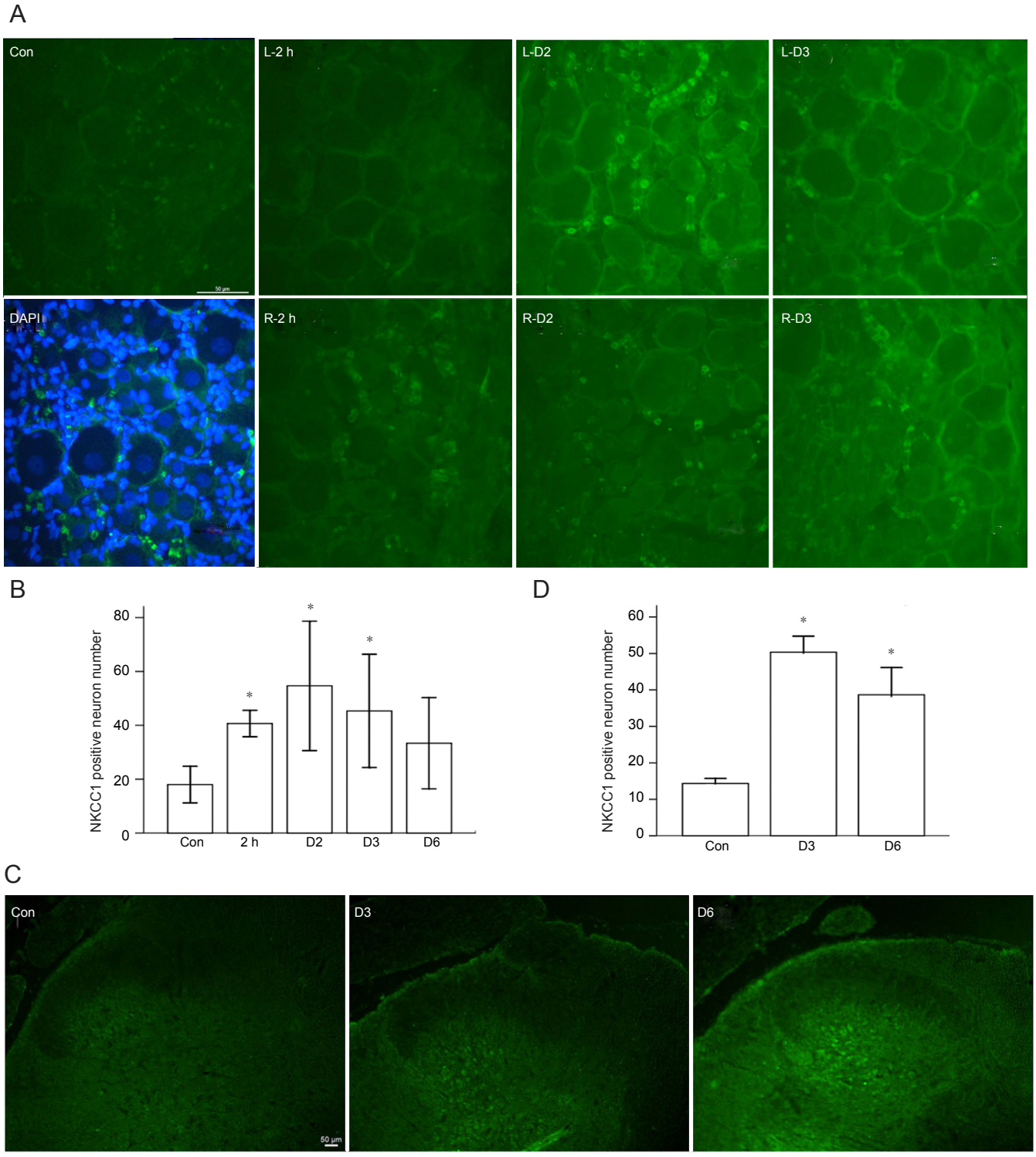


**Figure 2 Sodium-potassium-chloride co-transporter 1 (NKCC1) immunoreactivity increased in spinal dorsal root ganglion and dorsal horn following incision.**

(A) NKCC1 expression increased in $L_5$ dorsal root ganglion (DRG) after incision. NKCC1 immunoreactivity was indicated by fluorescein isothiocyaute (FITC)-conjugated IgG (green). Con: Weak NKCC1 immunoreactivity was observed in intact rats. DAPI: Left $L_5$ DRG at 3 days after incision. NKCC1 and nuclei double staining showed the membrane-associated expression in DRG neurons. L-2h, R-2h, L-D2, R-D2, L-D3, R-D3: NKCC1 immunoreactivity in the left and right $L_5$ DRG of rat at 2 hours, 2 days, and 3 days following incision. Scale bar: 50 μm. (B) NKCC1 immunoreactive neuron quantification in ipsilateral DRG. One-way analysis of variance followed by Levene's *post hoc* test was used for pairwise comparisons. (C) NKCC1 immunoreactivity increased in left dorsal horn of $L_{4–5}$ spinal cord after incision. NKCC1 immunoreactivity was indicated by FITC-conjugated IgG. Con: Weak NKCC1 IR was observed in deep layers of dorsal horn in intact rats. D3, D6: NKCC1 immunoreactivity increased in the deep layers of ipsilateral dorsal horn at 3 and 6 days following incision. Scale bar: 50 μm. (D) NKCC1 immunoreactive neuron quantification in ipsilateral dorsal horn of $L_{4–5}$ spinal cord, and one-way analysis of variance followed by Levene's *post hoc* test was used for pairwise comparisons. (B, D) Data were expressed as mean ± SD. $n = 6$, $*P < 0.05$, *vs.* control group.

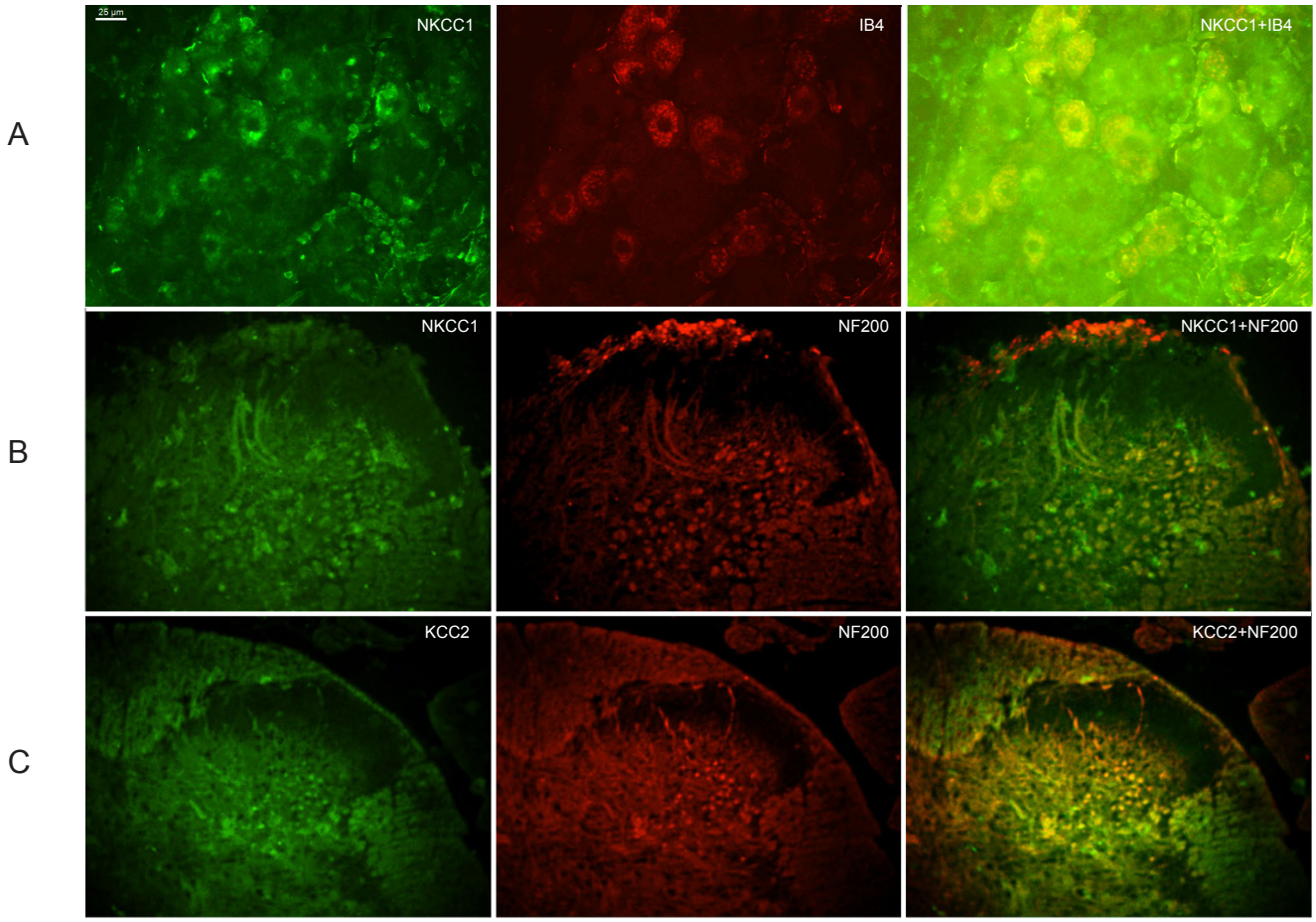


**Figure 4 Sodium-potassium-chloride co-transporter 1 (NKCC1)/potassium-chloride co-transporter 2 (KCC2) co-staining with C-fiber and A-fiber neuron markers.**
(A) NKCC1 expressed in C-fiber neurons in dorsal root ganglion. Green: NKCC1; red: isolectin B4 (IB4), marker of C-fiber neuron; yellow: overlay of NKCC1 and IB4. NKCC1 expressed in most dorsal root ganglion neurons, especially in C-fiber neurons. (B) NKCC1 expressed in A-fiber neurons in the dorsal horn. Green: NKCC1; red: neurofilament 200 (NF200), marker of A-fiber neuron; yellow: overlay of NKCC1 and NF200. NKCC1 was significantly expressed in A-fiber neurons in deep layers. (C) KCC2 expressed in A-fiber neurons in dorsal horn. Green: KCC2; red: NF200, marker of A-fiber neuron; yellow: overlay of KCC2 and NF200. KCC2 was predominantly expressed in deep A-fiber neurons. Scale bar: 25 μm.

and DAPI, we could not agree that, as reported before, all the NKCC1 signal around the large-diameter neurons were from satellite glial cells (Price et al., 2006). We consider that NKCC1 expression in the large Aβ fiber afferent neurons might be related to the effect of the NKCC1 inhibitor on touch-evoked pain. KCC2 mRNA was not found in dorsal root ganglion (Kanaka et al., 2001; Price et al., 2006), and thus we did not find KCC2 immunoreactivity in dorsal root ganglion. We therefore agree that no KCC2 expression occurs in dorsal root ganglion neurons, and this finding may be one of the reasons for the high intracellular chloride concentration seen in dorsal root ganglion neurons (Mao et al., 2012).

As reported, KCC2 mRNA and NKCC1 mRNA was detected throughout the dorsal horn, with KCC2 mRNA showing greater expression in this region (Price et al., 2006). We also found much stronger KCC2 immunoreactivity than NKCC1 in the deep layers. Furthermore, KCC2 expression was only detectable in the SG whereas intense KCC2 mRNA, no detectable NKCC1 expression in the SG, and little NKCC1 mRNA was noted in the intact rats. By contrast, both KCC2 and NKCC1 immunoreactivity appeared increased in the SG after incision, regardless of an increase or decrease in expression in the deep layers of the dorsal horn. We doubted that the NKCC1 and KCC2 immunoreactivity in SG was from the central terminals of primary afferent neurons, but this theory needs to be proven by further studies.

The change of spinal NKCC1 and KCC2 expression after incision was in accordance with our last pain behavior results using the NKCC1 and KCC2 inhibitor furosemide and results of the NKCC1 selective inhibitor bumetanide in this experiment. Being chloride transporters, CCCs play a major role in controlling responses mediated by GABAA receptors (Price et al., 2005, 2009). In dorsal root ganglion neurons, GABA-A receptor activation is depolarizing because of a slightly higher intracellular $Cl^-$ concentration ($[Cl^-]_i$), which leads to primary afferent depolarization. Under normal conditions, primary afferent depolarization shunts the mag-

nitude of incoming action potentials, leading to presynaptic inhibition. However, under pathological conditions, primary afferent depolarization might be enhanced to generate action potentials, which is hypothesized to be a potential mechanism for allodynia (Price et al., 2005). Our results suggest that the slightly higher $[Cl^-]_i$ in dorsal root ganglion neurons is due to predominant expression of NKCC1 under physiological conditions, and after incision-increased NKCC1 expression is involved in the mechanism of production of action potential from primary afferent depolarization. The inhibition of hyperalgesia and allodynia after incision by the CCC inhibitor furosemide and bumetanide could be explained partly by the blocking of increased NKCC1 function in dorsal root ganglion.

We also found NKCC1 immunoreactivity increased and KCC2 immunoreactivity reduced in the deep laminae of the dorsal horn. Unlike primary afferent neurons, spinal dorsal horn neurons maintain low $[Cl^-]_i$ because of their relatively high level of KCC2 expression in the adult under normal conditions, and GABAA receptor mediated inhibition acting postsynaptically on dorsal horn neurons (Price et al., 2005, 2009; Blaesse, 2009). Downregulation of KCC2 or upregulation of NKCC1 that result in higher $[Cl^-]_i$ in dorsal horn neurons might disinhibit the nociceptive pathway by transferring the low threshold input to nociceptive neurons that underlies the mechanism of hyperalgesia (Price et al., 2005). It is evidenced that sensitization of dorsal horn neurons can be reduced by NKCC1 blockade by *in vivo* electrophysiological recordings (Pitcher and Cervero, 2010). We suggested that NKCC1 overexpression and lower KCC2 expression in dorsal root following incision might contribute to postoperative hyperalgesia, and intrathecal bumetanide could reduce hyperalgesia by inhibition of NKCC1 function.

After incision, changes in spinal NKCC1 and KCC2 expression may alter neuronal excitability and GABAergic responses, thereby modulating nociceptive gating and pain sensitivity. Intrathecal administration of NKCC1 inhibitor has an analgesic effect on incisional pain. These results underscore the potential of NKCC1 blockers as a therapeutic strategy for postoperative pain management.

**Author contributions:** *He YB designed this study, performed the experiments, and wrote this paper. Xu SY designed this study and revised the paper. Huang JJ performed the experiments. Gong QJ analyzed the data and wrote the paper. All authors approved the final version of this study.*

**Conflicts of interest:** *None declared.*

## References

Aasvang E, Kehlet H (2005) Chronic postoperative pain: the case of inguinal herniorrhaphy. Br J Anaesth 95:69-76.

Blaesse (2009) Cation-chloride cotransporters and neuronal function. Neuron 61:820-838.

Bolay H, Moskowitz MA (2002) Mechanisms of pain modulation in chronic syndromes. Neurology 59:S2-7.

Brennan TJ (2011) Pathophysiology of postoperative pain. Pain 152:S33-40.

Brennan TJ, Vandermeulen EP, Gebhart GF (1996) Characterization of a rat model of incisional pain. Pain 64:493-501.

Chamma I, Chevy Q, Poncer JC, Levi S (2012) Role of the neuronal K-Cl co-transporter KCC2 in inhibitory and excitatory neurotransmission. Front Cell Neurosci 6:5.

Chaplan SR, Bach FW, Pogrel JW, Chung JM, Yaksh TL (1994) Quantitative assessment of tactile allodynia in the rat paw. J Neurosci Methods 53:55-63.

Funk K, Woitecki A, Franjic-Wurtz C, Gensch T, Mohrlen F, Frings S (2008) Modulation of chloride homeostasis by inflammatory mediators in dorsal root ganglion neurons. Mol Pain 4:32.

Gilbert D, Franjic-Wurtz C, Funk K, Gensch T, Frings S, Mohrlen F (2007) Differential maturation of chloride homeostasis in primary afferent neurons of the somatosensory system. Int J Dev Neurosci 25:479-489.

Granados-Soto V, Arguelles CF, Alvarez-Leefmans FJ (2005) Peripheral and central antinociceptive action of Na+-K+-2Cl- cotransporter blockers on formalin-induced nociception in rats. Pain 114:231-238.

Haas M, Forbush B, 3rd (1998) The Na-K-Cl cotransporters. J Bioenerg Biomembr 30:161-172.

Hargreaves K, Dubner R, Brown F, Flores C, Joris J (1988) A new and sensitive method for measuring thermal nociception in cutaneous hyperalgesia. Pain 32:77-88.

Hasbargen T, Ahmed MM, Miranpuri G, Li L, Kahle KT, Resnick D, Sun D (2010) Role of NKCC1 and KCC2 in the development of chronic neuropathic pain following spinal cord injury. Ann N Y Acad Sci 1198:168-172.

He Y, Ji W, Huang H (2011) Effect of the cation-chloride cotransporter inhibitor furosemide in a rat model of postoperative pain. Pain Med 12:1427-1434.

Imani F, Rahimzadeh P (2012) Gabapentinoids: gabapentin and pregabalin for postoperative pain management. Anesth Pain Med 2:52-53.

Kanaka C, Ohno K, Okabe A, Kuriyama K, Itoh T, Fukuda A, Sato K (2001) The differential expression patterns of messenger RNAs encoding K-Cl cotransporters (KCC1,2) and Na-K-2Cl cotransporter (NKCC1) in the rat nervous system. Neuroscience 104:933-946.

Kehlet H, Jensen TS, Woolf CJ (2006) Persistent postsurgical pain: risk factors and prevention. Lancet 367:1618-1625.

Lavand'homme P (2006) Perioperative pain. Curr Opin Anaesthesiol 19:556-561.

Mao S, Garzon-Muvdi T, Di Fulvio M, Chen Y, Delpire E, Alvarez FJ, Alvarez-Leefmans FJ (2012) Molecular and functional expression of cation-chloride cotransporters in dorsal root ganglion neurons during postnatal maturation. J Neurophysiol 108:834-852.

Payne JA, Rivera C, Voipio J, Kaila K (2003) Cation-chloride co-transporters in neuronal communication, development and trauma. Trends Neurosci 26:199-206.

Pitcher MH, Cervero F (2010) Role of the NKCC1 co-transporter in sensitization of spinal nociceptive neurons. Pain 151:756-762.

Price TJ, Cervero F, de Koninck Y (2005) Role of cation-chloride-cotransporters (CCC) in pain and hyperalgesia. Curr Top Med Chem 5:547-555.

Price TJ, Hargreaves KM, Cervero F (2006) Protein expression and mRNA cellular distribution of the NKCC1 cotransporter in the dorsal root and trigeminal ganglia of the rat. Brain Res 1112:146-158.

Price TJ, Cervero F, Gold MS, Hammond DL, Prescott SA (2009) Chloride regulation in the pain pathway. Brain Res Rev 60:149-170.

Vadivelu N, Mitra S, Narayan D (2010) Recent advances in postoperative pain management. Yale J Biol Med 83:11-25.

Wu CL, Raja SN (2011) Treatment of acute postoperative pain. Lancet 377:2215-2225.

Zahn PK, Umali E, Brennan TJ (1998) Intrathecal non-NMDA excitatory amino acid receptor antagonists inhibit pain behaviors in a rat model of postoperative pain. Pain 74:213-223.

Zahn PK, Sluka KA, Brennan TJ (2002a) Excitatory amino acid release in the spinal cord caused by plantar incision in the rat. Pain 100:65-76.

Zahn PK, Pogatzki EM, Brennan TJ (2002b) Mechanisms for pain caused by incisions. Reg Anesth Pain Med 27:514-516.

Zhang W, Liu LY, Xu TL (2008) Reduced potassium-chloride co-transporter expression in spinal cord dorsal horn neurons contributes to inflammatory pain hypersensitivity in rats. Neuroscience 152:502-510.

*Copyedited by Apricò K, Robens J, Wang J, Li CH, Song LP, Zhao M*